

# Microfacies and diagenetic evolution of the limestones of the upper part of the Crato Formation, Araripe Basin, northeastern Brazil

Flávia Araújo de Arruda Cabral<sup>1\*</sup> , Ana Cláudia da Silveira<sup>1</sup> , Germano Mário Silva Ramos<sup>1</sup> ,  
Tiago Siqueira de Miranda<sup>2</sup> , José Antonio Barbosa<sup>2</sup> , Virgínio Henrique de Miranda Lopes Neumann<sup>2</sup> 

## Abstract

This paper presents the results of a petrographic and diagenetic study of the laminated limestones of the upper part of the Aptian to Albian Crato Formation, northeast of Brazil. The applied techniques were optical microscopy, cathodoluminescence and scanning electron microscopy (SEM) coupled to a wavelength-dispersive spectrometer (WDS). Petrographic analysis has revealed that most of the laminated limestones are calcilitites with a dominance of a micritic matrix, indicating a low-energy depositional environment. Microstructures such as microfaults, microfractures, microslumps, and loop bedding were observed. Based on textural, structural and paleontological features, seven microfacies were recognized: massive limestone, limestone with parallel laminations, limestone with undulated laminations, limestone with slumps, limestone with loop bedding, limestone with ostracods and limestone with peloids. In addition, the processes of cementation, dissolution, replacement, recrystallization and compaction, which are related to different diagenetic stages, were also recognized. The diagenetic constituents found in the sections include calcite, pyrite, silica and sulfates. We can conclude that a large part of the microstructures (microfaults, microfractures, microslumps and loop bedding) can be related to local seismicity, probably due to the reactivation of the Patos Shear Zone. The diagenetic constituents indicate an early to late diagenesis (eogenetic, mesogenetic and telogenetic stage).

**KEYWORDS:** Crato Formation; laminated limestones; diagenesis; Araripe Basin.

## INTRODUCTION

Since the discovery of hydrocarbons in carbonate rocks of the so-called pre-salt layer in the marginal basins of Brazil, the interest increased in the search for rocky exposures as possible analogues of these reservoirs. The upper part of the Aptian to Albian Crato Formation, a well-exposed and preserved carbonate succession in the Araripe Basin (NE Brazil), is probably a good analogue. These carbonate rocks present features interpreted as algalic growth (Neumann 1999, Catto *et al.* 2016), similar to those occurring in the reservoir rocks of the pre-salt layer, as well as structures that can be interpreted only as event products of diagenesis (Neumann 1999). In this sense, based on petrographic, microfacies and microstructure analysis, an attempt is made, in this paper, to understand some of the issues related to the origin and diagenesis of these carbonate rocks.

The Araripe Basin is located in the interior of northeastern Brazil, occupying part of the states of Pernambuco, Ceará and Piauí, and covers an area of approximately 9,000 km<sup>2</sup>, consisting of one of the most extensive interior basins in northeastern Brazil. It is located in the Piancó-Alto Brígida Terrain (Santos *et al.* 2004), in the western portion of the Transversal Subprovince of the Borborema Province. Its origin and evolution are related to the tectonic events of the Late Cretaceous, leading to the rupture of the Supercontinent Gondwana and the subsequent formation of the South Atlantic Ocean.

The structural configuration of this basin includes the tabular strata that formed the Araripe Plateau. This plateau is composed of the Barbalha, Crato, Ipubi and Romualdo formations and represents the post-rift sequences of the Araripe Basin (Assine 2007).

The Crato Formation represents the second lacustrine phase of the post-rift supersequence of the basin, which consists of six limestone units (informally called C1 to C6), according to Neumann (1999), deposited in the central and marginal zones of the basin forming carbonate bodies with different thicknesses and varied lateral extension. These six limestone units, 20 to 70 m in thickness, are in the lower part of the Santana Group and comprise two lithofacies, the rhythmite clay/limestone and the laminated limestone (Neumann 1999). These rocks are micritic and were deposited in internal lacustrine calm environments during the Aptian-Albian time-interval (Lima 1978, 1980, Hashimoto *et al.* 1987, Pons *et al.* 1990, Berthou *et al.* 1994, Coimbra *et al.* 2002, Batten 2007).

<sup>1</sup>Geosciences Post-Graduation Program, Center of Technology and Geosciences, Universidade Federal de Pernambuco – Recife (PE), Brazil. E-mail: flavia\_araujo7@hotmail.com, silveira.aninhac@gmail.com, nonogermano@gmail.com

<sup>2</sup>Laboratory of Sedimentary and Environmental Geology, Department of Geology, Center of Technology and Geosciences, Universidade Federal de Pernambuco – Recife (PE), Brazil. E-mail: tiagooufpe@gmail.com, barboant@hotmail.com, neumann@ufpe.br

\*Corresponding author.



The carbonate section of the Crato Formation in the Araripe Basin has invariably been considered to be lacustrine (Neumann 1999, Neumann & Cabrera 1999), except for a single reference that reports the existence of marine forms of foraminifera (Arai 2012). Therefore, it is interpreted that, due to its geographic position in the continent, the marine entry in the Araripe Basin occurred with relative delay in relation to the marginal basins.

The laminated limestones are intercalated with a series of clays, siltstones and sandstones. According to Martill & Heimhofer (2007), the Crato Formation can be divided into four different members, including from the base to the top the Nova Olinda, Caldas, Jamacaru and Casa de Pedra members, but this subdivision was not adopted in this work.

The objective of this paper is to characterize the laminated limestones in the upper part (unit C6) of the Crato Formation in sedimentological, petrographic, microfaciological, microstructural and diagenetic terms.

## GEOLOGICAL SETTING

The Araripe Basin is part of the Transversal Subprovince of the Borborema Province, located between the Pernambuco and Patos Shear Zones.

The structural configuration of this basin covers the tabular strata that formed the Araripe Plateau. This E-W-elongated plateau is an outstanding geomorphologic feature of northeast Brazil. It consists of sedimentary units of the post-rift sequence of the Araripe Basin, unconformably overlying older units or directly in angular unconformity upon the crystalline basement, a common configuration in the western portion of the basin, as shown in Figure 1.

According to Ponte and Appi (1990), Assine (1990, 1992) and Ponte and Ponte Filho (1996), the Araripe Basin can be subdivided into sequences linked by regional unconformities, reflecting distinct tectonic phases in the basin. Assine (2007) integrated these different proposals, identifying four large units bounded by unconformities:

- a Paleozoic sequence represented by the alluvial deposits of the Cariri Formation and characterized by medium to coarse grained sandstones of Silurian-Devonian age (Beurlen 1962, Assine 1992, 2007, Arai 2006), which is interpreted as the residual deposits of a large intracratonic basin;
- the Upper Jurassic pre-rift supersequence that corresponds to the Brejo Santo (predominantly pelites, red beds) and Missão Velha (coarse- to fine-grained sandstones and conglomeratic sandstones) formations;
- the rift supersequence represented by the Lower Cretaceous Abaiara Formation formed by a succession of laterally discontinuous sandstones intercalated with calciferous shales of variegated coloration (Fambrini *et al.* 2012);
- the post-rift supersequence, subdivided into two sequences, the post-rift I sequence of Aptian-Albian age, corresponding to the Barbalha Formation and the Santana Group (Crato, Ipubi and Romualdo formations) according to Assine *et al.* (2014), and the post-rift II sequence of Albian-Cenomanian age, which is characterized by alluvial sediments of the Araripina and Exu formations, indicative of tectonic reactivation in this time interval.

## MATERIALS AND METHODS

The classification of the limestone and the interpretation of the microfacies, the diagenetic evolution and the depositional environments are based on field observations (eight outcrops), samples and thin sections. Lithologic, sedimentological and structural descriptions were made. Samples were collected to prepare thin sections for subsequent petrographic study under optical microscope, cathodoluminescence and scanning electron microscopy (SEM) coupled to a wavelength-dispersive spectrometer (WDS).

The laboratory analysis is comprised of petrographic descriptions of 44 thin sections using a model BX-41 Olympus petrographic microscope at the Department of Geology, at Universidade Federal de Pernambuco (UFPE). At this stage, it was possible to describe the textural and structural features, as well as to identify the mineralogical (cement, grains and matrix) and paleontological compositions. Some types of porosity and diagenetic features were also identified.

Cathodoluminescence analysis was used in the study of diagenetic processes, to highlight the presence of fractures and the evolution of porosity in rocks and to recognize the different generations of cement. The study was conducted using a Cambridge Image Technology Ltd. (CITL) CL8200 model coupled to an optical microscope.

A JEOL KAL 6460 SEM with a wavelength-dispersive spectrometer from the Nanostructure Laboratory (LDN) was also used to aid in the identification and semiquantitative analysis of chemical elements.

The integrated analysis allowed the classification of the limestones in the upper part of the Crato Formation using the classification of Grabau (1904) and Dunham (1962). In addition, it was possible to characterize the seven microfacies of these laminated limestones based on textural and microstructural features and fossil contents, and to define the diagenetic evolution of these rocks.

## RESULTS

### Macroscopic analysis

The studied outcrops are located in the northern part of the Araripe basin, in the upper part of the Crato Formation. Macroscopically, these limestones are fine-grained, forming horizontal tabular layers that are locally intercalated with terrigenous rocks, such as shale and claystone (Figs. 2A and 2B). Limestones are mainly laminated with alternating light and dark laminae, of beige and brown color, respectively, sometimes being bluish. However, they have also been observed in massive and stratified forms (Fig. 2C).

Regarding the structural aspects, it has been observed that these rocks are intensely fractured and cemented by calcite and silica in some outcrops, but some unfilled fractures also occur. In addition to several shear fractures, they displace the laminations in the laminated limestones. Microfaults have also been observed, and they are mostly of the normal type.

Locally, calcite veins with cone-in-cone structures (Fig. 2D) have been observed as evidence of the recrystallization process. Salt pseudomorphs, such as hopper-faced halite, have also been seen (Fig. 3A).

It was possible to verify the presence of micropores caused by dissolution. Some of these pores are cemented by recrystallized calcite or quartz, and geode structures formed by calcite may also occur.

In some outcrops, where the surface of the upper part of the C6 level can be observed, it was possible to note that the limestone laminae showed undulations (Fig. 3B) and a botryoidal surface characterized by an irregular and wavy feature which is associated with pedogenetic or diagenetic processes. In addition, a silicification process was perceived in these portions (Fig. 3C) in the macroscopic analysis and confirmed by microscopy.

Locally, a collapse-breccia with various fragments of laminated limestone cemented by carbonatic and siliceous matrix was observed (Fig. 3D).

### Microfacies of level C6 of the Crato Formation

Only the lithofacies of the laminated limestone was observed, since it refers to the upper part of the Crato Formation and, in this case, the C6 level proposed by Neumann (1999). This is the main and most representative carbonate lithofacies occurring in the Crato Formation. It is represented in this work by beige to brown and sometimes gray to blue laminated limestone, with parallel laminations, locally undulated and with the presence of sliding

structures (microslumps), microfaults, microfractures, loop bedding, ostracods and peloids.

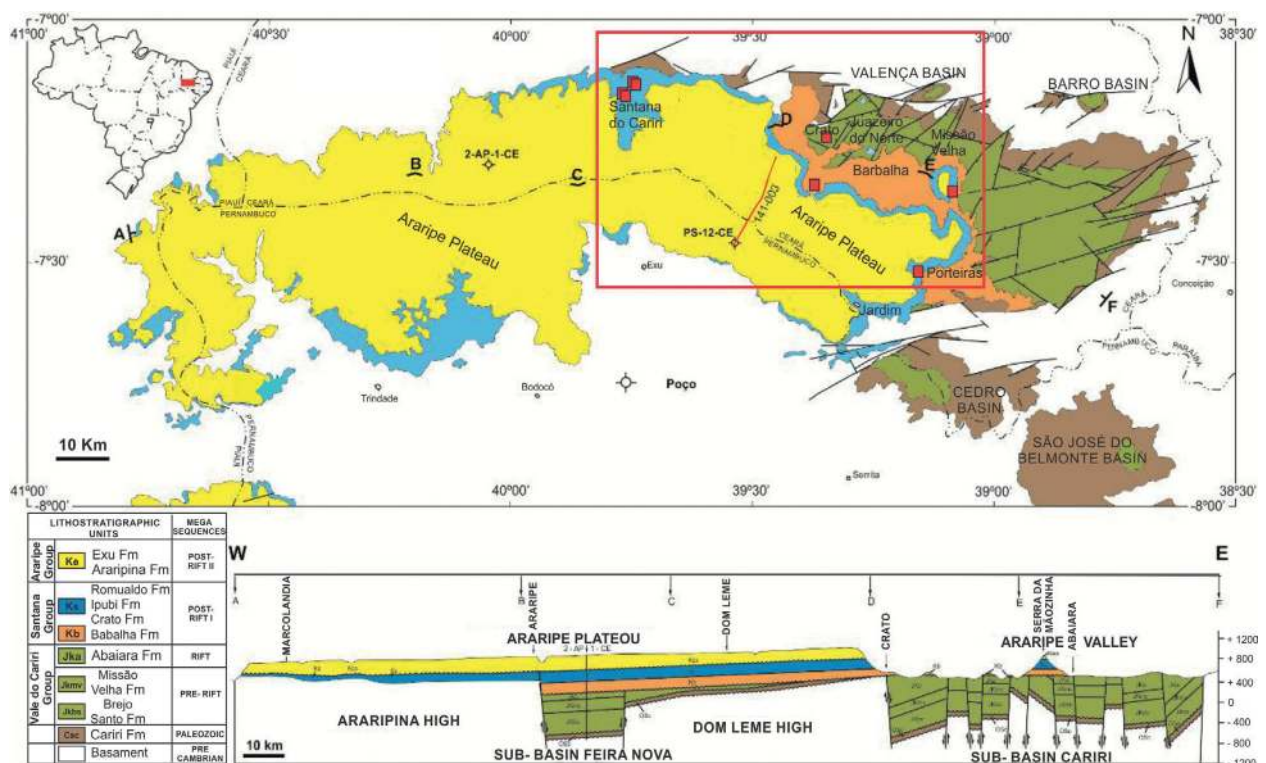
The microscopic characteristics allowed us to characterize seven microfacies (m1 to m7) according to texture, structures and bioclastic content: massive limestone, limestone with parallel laminations, limestone with undulated laminations, limestone with slumps, limestone with loop bedding, limestone with ostracods and limestone with peloids (Tab. 1).

### Massive limestone microfacies (m1)

The massive limestone microfacies (m1) consists of a carbonate mud composed of micritic calcite with colors ranging from beige to light brown, usually without visible lamination under the microscope, and contains, locally, framboidal pyrite and iron oxide stains (Fig. 4). Tectonic features can also be observed, such as microfractures filled/cemented by calcite and/or silica. Primary or secondary porosities are typically absent in this microfacies.

### Limestone with parallel laminations microfacies (m2)

This is the microfacies with the largest occurrence in these limestones. It is represented by limestone with millimeter-thick parallel laminae, organic matter, opaque minerals (framboidal pyrite), and iron oxide resulting from the alteration of these pyrites. In addition, several filled or unfilled microfractures were observed. The beige laminae are composed of micritic calcite, whereas the dark one is more often defined by the presence of opaque minerals, iron oxide and organic matter (Fig. 5). Organic matter, silica and calcite were also observed filling the microfractures.



Source: modified from Assine *et al.* (2014).

**Figure 1.** Simplified geological map of the Araripe Basin with emphasis on the study area and studied outcrops (red square).

*Limestone with undulated laminations microfacies (m3)*

This microfacies was found in only two outcrops located at the contact of the Crato and Ipubi formations. It is characterized by crenulated organic lamellae, which in most cases are wavy and deformed (Fig. 6). Framboidal

pyrite, iron oxide and various fractures filled with fibrous calcite were also observed. In addition, silica (cryptocrystalline quartz, megaquartz and chalcedony) and sulfates (gypsite, anhydrite and barite) were found to occur as substitutions.

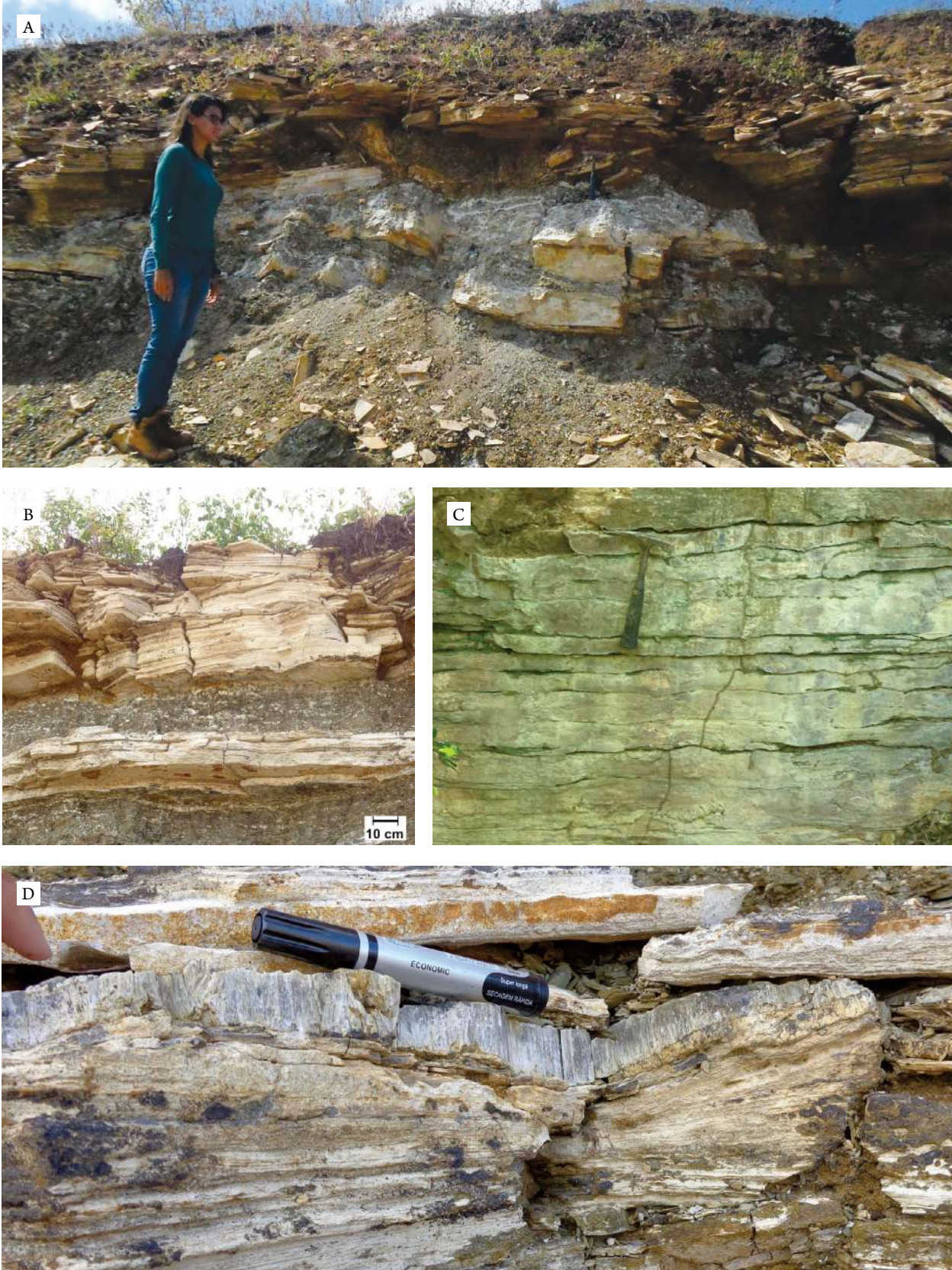


**Figure 2.** (A) Outcrop (Aurélio's Quarry) with laminated limestone intercalated with claystone; (B) laminated limestone intercalated with shale in Três Irmãos Quarry; (C) fractured stratified limestone in outcrop located in Abaiara; (D) calcite vein with a cone-in-cone structure.

**Limestone with slumps microfacies (m4)**

This microfacies presents the same characteristics of the m2 microfacies, but with smooth laminations and the presence of sliding features or microslumps in soft-sediment (Fig. 7).

**Limestone with loop bedding microfacies (m5)**

In this microfacies, laminated limestone is produced with microstructures called loop bedding, consisting of “small groups of laminae that are sharply constricted or that terminate at intervals, giving the effect of long, thin

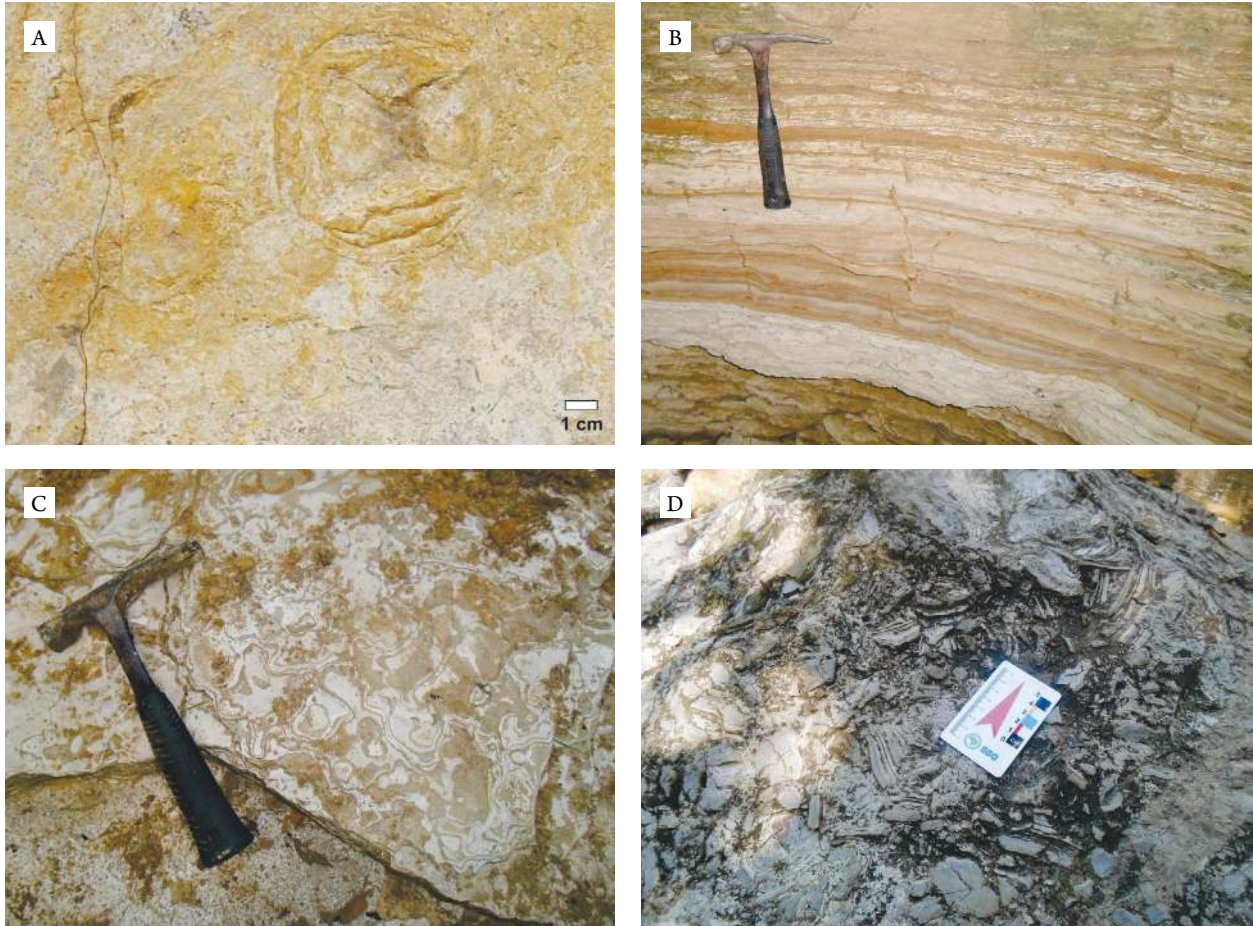


**Figure 3.** (A) Laminated limestone with a halite pseudomorph (center of the image), in the form of a star, in outcrop of Santana do Cariri; (B) outcrop of limestone with its wavy bands, located in Porteiras; (C) silicified laminated limestone showing a botryoidal surface (located in Porteiras); (D) collapse-breccia with laminated limestone fragments in Porteiras.

**Table 1.** Microfacies of the limestones from the upper part of the Crato Formation.

Microfacies	Diagnosis	Interpretation
m1	Carbonate mud composed of micritic calcite with colors ranging from beige to light brown	Limestone preserved in calm environment with micrite formed by <i>in situ</i> precipitation
m2	Limestone with millimeter plane-parallel laminae	Limestone preserved in calm environment, without disturbance in the inner lake
m3	Limestone with crenulated organic lamellae and pyrite-substituted that are in most cases wavy and deformed	Lake with high salinity with lamination consisting of algae mats and with desiccation period
m4	Limestone with microslumps	Event of slumping in soft-sediment
m5	Laminated limestone with microstructures similar to sedimentary boudinage (loop bedding)	Features related to seism affecting soft-sediments and also generated diagenetically by overload
m6	Limestone with ostracods	A probable low-energy environment, since the ostracodes usually exhibit articulated valves
m7	Limestone with peloids	Probably occur anywhere of the photic zone in the lake

loops or links of a chain” (Bates & Jackson 1980), similar to sedimentary boudinage. The loop bedding can be classified as simple or complex. However, here, we have observed only simple loop bedding, generated diagenetically by overload (Fig. 8).

#### *Limestone with ostracods microfacies (m6)*

This microfacies was found in both laminated and massive limestones. Bioclasts identified as ostracods have been observed, the interior of which one filled by micritic or spar calcite or by pyrite, which mostly occurs with whole and articulated valves that suggest low energy sedimentation, but locally they have compaction features, with disarticulated and flattened valves. These ostracods are replaced by micritic and/or sparry calcite (Figs. 9A and 9B) and by pyrite (Figs. 9C and 9D).

#### *Limestone with peloids microfacies (m7)*

This microfacies is poorly represented in the thin sections studied. A level of millimetric peloids having circular and ellipsoidal forms was observed without internal structure and composed of micrite and distributed in a micritic matrix. The origin of these peloids may relate to the alteration of bioclasts (Fig. 10).

### Diagenetic processes

Diagenesis typically involves a variety of physical and chemical processes. The most common and identified here are dissolution, cementation, replacement, recrystallization and compaction.

The dissolution process is represented by secondary porosities (Fig. 11A), which are represented by the vuggy and fenestral types of porosities and are classified according to Choquette and Pray (1970).

With respect to cementation (Fig. 11B), calcite cements were found to occur in sparry, prismatic and fibrous forms (Fig. 12A and 12B), in addition to silica, both of which filled fractures.

In these limestones in the upper part of the Crato Formation, several mineral phases were observed, which replaced these carbonates. These substitutions were then referred to as pyritization, silicification and sulfation.

The pyritization is characterized by the most common iron sulfide ( $\text{FeS}_2$ ) found in carbonate rocks, whose presence is very often found in all the microfacies defined herein. It is represented by microcrystalline and framboidal pyrite, which usually forms anhedral replacement masses. It is produced in a fairly distributed manner in the rocks and locally replaces organic matter and some bioclasts, in this case, ostracods (Fig. 12C).

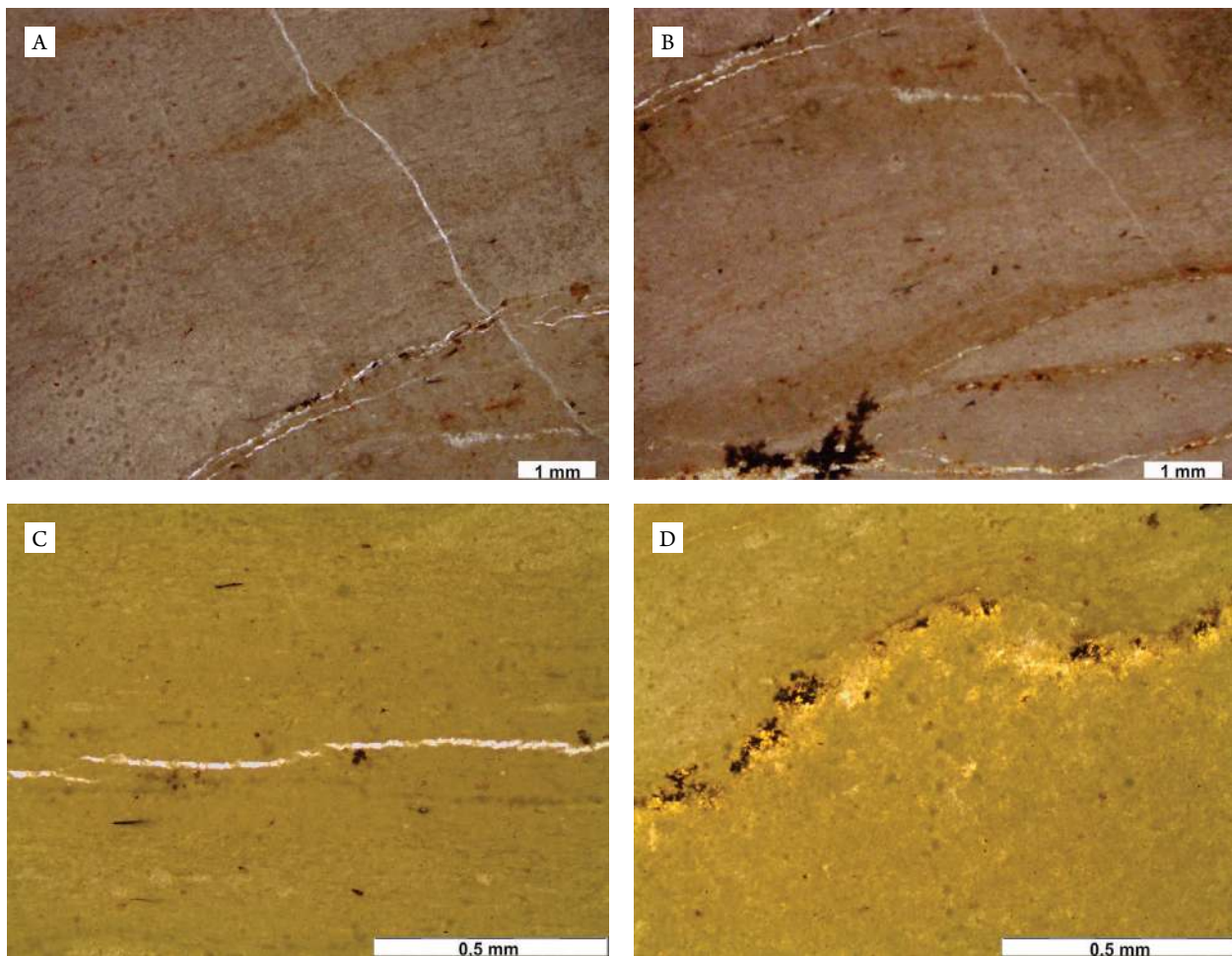


**Figure 4.** Massive limestone microfacies: (A) and (B) carbonate mud with diagonal fractures filled by calcite; (C) carbonate mud with horizontal fracture; (D) carbonate mud with framboidal pyrite. Photomicrographs: parallel nicols.

The silicification process is characterized by silica ( $\text{SiO}_2$ ), a diagenetic mineral phase that is very common in carbonate rocks and can occur as cement or as a replacement of the original material. Although there are several diagenetic species of silica, only cryptocrystalline quartz (chert), megaquartz and chalcedony (fibrous and radial forms and spherulitic structures) were observed (Fig. 12D).

Other minerals that are present in the contact between the Crato and Ipubi formations are sulfates (Figs. 12E and 12F), thus giving origin to the sulfation process, which is represented by the occurrence of gypsum, barite (Fig. 13) and anhydrite.

The recrystallization process was observed locally in these limestones, where micritic calcite change occurs, there by generating sparry calcite. These calcites occur as fracture fill.

Finally, compaction was observed, exhibiting only mechanical compaction (Bathurst 1986). It is defined by deformation features in the clay-organic laminations, in addition to the presence of some displaced and sometimes flattened valves of ostracods.

## DISCUSSION

The macro- and microscopic analysis in this research confirmed the sedimentological and structural aspects previously described by Neumann (1999) and Silva (2003) as the

dominance of micritic calcite, microfaults, microslumps and loop bedding structures.

In general, these lacustrine limestones of Aptian-Albian age were classified as calcilutites, due to granulation, according to the classification of Grabau (1904). As it was observed, these rocks are composed of a micritic matrix with less than 10% grains and can be classified as mudstones according to Dunham (1962).

High luminescence in these lacustrine limestones was observed in all thin sections examined using cathodoluminescence analysis. This high luminescence could be associated with the relatively high Mn/Fe ratio, typically obtained under reducing conditions during the early stage of burial diagenesis.

According to Heimhofer *et al.* (2010), the origin of the Crato Formation carbonates is traditionally attributed to the chemical precipitation associated with clastic fine-grained sediments and is unaffected by any organic organism. Catto (2015) observed the presence of the organic matrix extracellular polymeric substance (EPS) in the laminated limestones of the Crato Formation and used this substance as a diagnostic criterion for the biotic influence on the precipitation of carbonate minerals. The last author has identified calcified organisms (filamentous and coccus bacteria, and cyanobacteria) and suggested

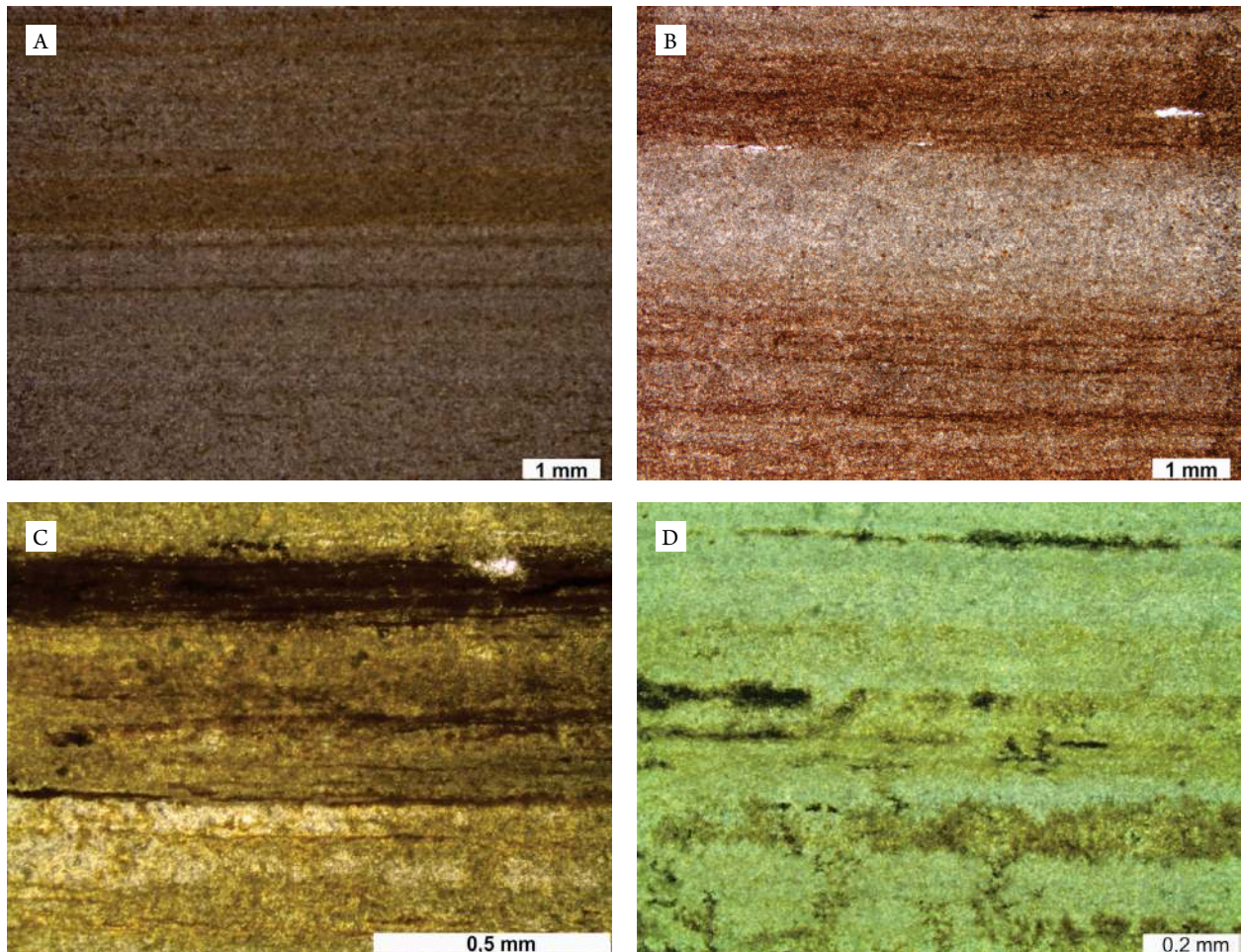


**Figure 5.** Limestone of the parallel laminations microfacies: (A) and (B) the dark bands are composed of microcrystalline calcite, organic matter and pyrite, while the light bands are constituted of microcrystalline calcite without pyrite. Evidence of recrystallization of calcite in the lower portion (lighter color) is seen in C. The dark stain in the lower part of D refers to an arboreal manganese. Photomicrographs: parallel nicols.

that the Crato Formation carbonates come from biologically induced precipitations.

In this study, some laminations similar to algae mats have been observed, as shown in the m3 microfacies. Therefore, the origin of these limestones could be bio-induced by algae growth, as observed in Catto (2015), and related to chemical precipitation (Heimhofer *et al.* 2010).

The organic laminations observed in the m3 microfacies are compound algae mats that represent a hypersaline environment, whose observed deformation has been related to a desiccation and compaction process acting on the lacustrine system.

The greatest importance of these carbonate rocks is their potential for the reservoir rocks, and here it has been observed that the outcrops of the carbonate rocks in the upper part of the

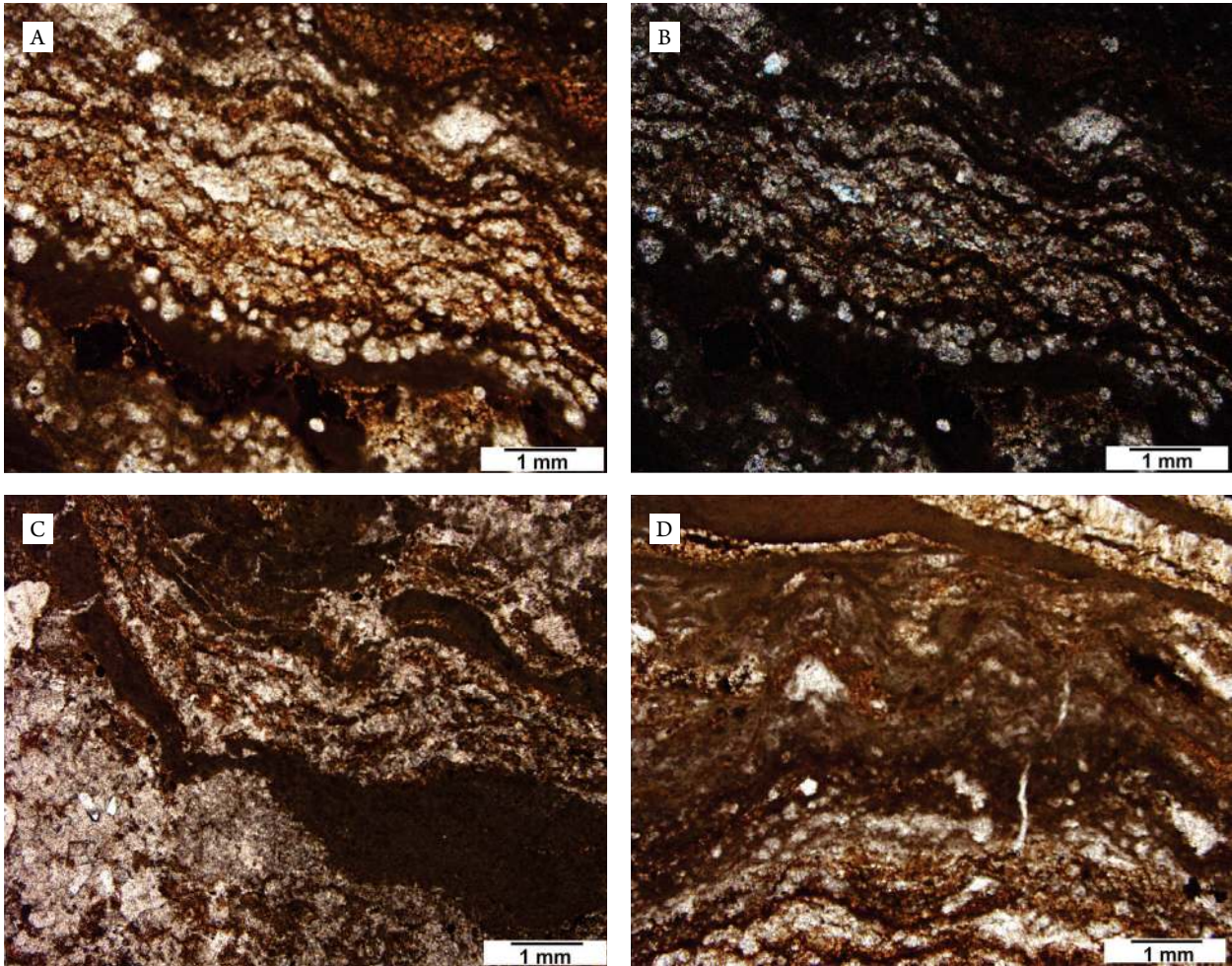


**Figure 6.** Limestone with undulated laminations microfacies: limestone with organic laminae, brownish-colored, crenulated and deformed with recrystallized calcite. Photomicrographs: (A) parallel nicols, (B) crossed nicols, (C) and (D) parallel nicols.

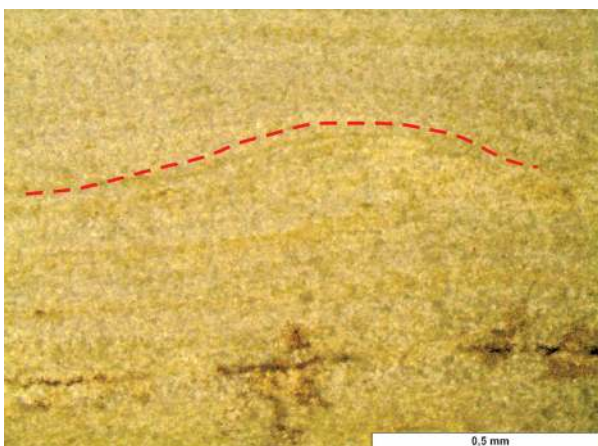


**Figure 7.** Limestone with slumps microfacies: microslumps located in the center of the illustration are highlighted by a dashed line. Photomicrograph: parallel nicols.

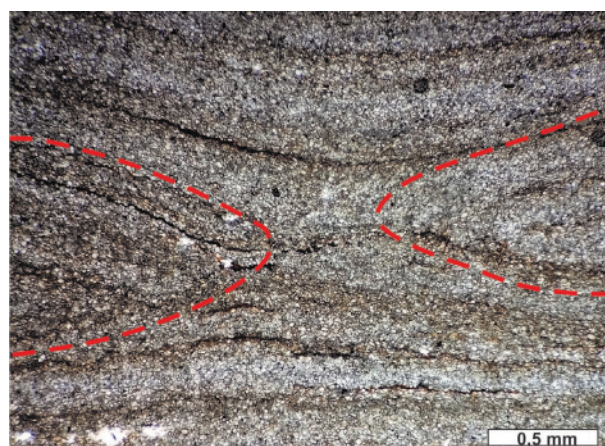


**Figure 8.** Limestone with loop bedding microfacies: laminated limestone with simple loop bedding highlighted by hatching contour. Photomicrograph: parallel nicols.



Crato Formation are quite fractured. However, a large part of these fractures are sealed. Hence, in addition to the fractures, the vuggy and fenestral porosities are also mostly cemented. Therefore, in this work, with respect to the potential of the reservoir rocks, the lithotypes of the upper part of the Crato Formation were characterized by a low grade of permeability and, thus, a low reservoir potential.

According to Miranda (2015), based on the geological and perm-porosity characteristics obtained for the laminated limestones in the upper part of the Crato Formation, it has been possible to classify them as an analogue of naturally fractured type 4 (Nelson 1987, 2001), in which the matrix has a medium to high primary porosity and low permeability, and the fractures are cemented. Thus, it could be classified as an unconventional reservoir of "tight" type (when porosity is associated with the microporosity). In general, Miranda (2015) considers these limestones to have a medium primary porosity and very low permeability, as well as to contain a series of fractures cemented by calcite that form a hydraulic barrier, as observed in this study.

The structural features observed in these laminated limestones are microslumps, loop bedding, microfractures and microfaults (Neumann 1999), which may be related to local seismicity occurring in the region and probably related to

the reactivation of the Patos Shear Zone, in the North of the Araripe Basin. This fact was also noted by Silva (2003), who recognized three deformational stages (D1, D2 and D3) in this unit. These microstructures were generated during the D1 event, brittle-ductile extensional, located in some thin limestone levels and are the result of small seismic pulses. Silva (2003) suggested that these structures occur in a few levels of the carbonate units, which may indicate sporadic events of seismic pulses over long time intervals, since some levels do not exhibit such characteristics.

Diagenesis was subdivided into three main stages: eodiagenetic, mesogenetic and telodiagenetic. Therefore, with the study of diagenetic processes, it was possible to determine the stage at which each event occurred.

Typical eodiagenetic features were observed, such as intergranular porosity in the micritic matrix and the presence of microcrystalline and framboidal pyrite ( $\text{FeS}_2$ ). Additionally, at this stage, the presence of sulfate minerals that form closer contact with the Ipubi Formation was observed.

A dissolution process was noticed that gave rise to a vuggy and fenestral secondary porosities that represents the mesogenetic stage. Additionally, cementation by silica and calcite was verified and also a process of silicification, which occurs in form as cryptocrystalline quartz, megaquartz and chalcedony.

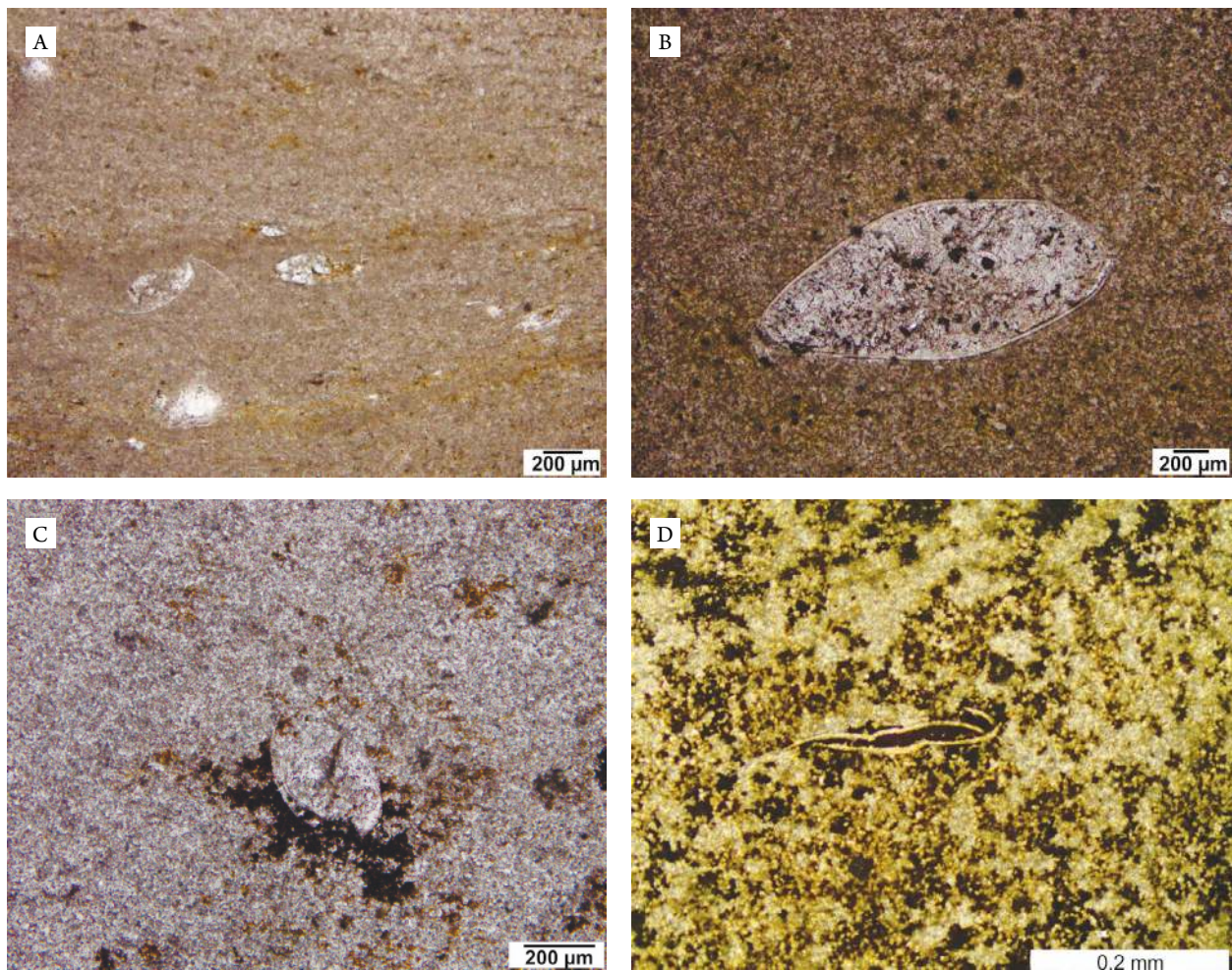


**Figure 9.** Limestone with ostracods microfacies: (A) replacement sometimes by spar calcite or so metimes by micritic calcite of ostracods; (B) ostracod with valves constituted by calcite and microcrystalline calcite inside; (C) ostracod with the beginning of pyritization; (D) ostracod flattened with a disarticulated valve and replaced with pyrite. Photomicrograph: parallel nicols.

At this stage, the recrystallization process was characterized by microfractures that are often sealed by blocky or fibrous calcite cement.

The telodiagenetic stage is represented by the presence of iron oxide, which were fairly observed in these limestones and are associated with the alteration of pyrite by oxidation processes.

According to Boggs Jr. (2009), the origin of silica can be essentially a product of dissolution by meteoric waters (weathering), dissolution of the skeletons of organisms, dissolution of quartz grains, pressure solution of quartz grains and release of silica by reactions between minerals, as occurs with clay minerals. In the case of the Crato Formation limestones, the origin is mainly related to meteoric water saturated in  $\text{SiO}_2$ , which, due

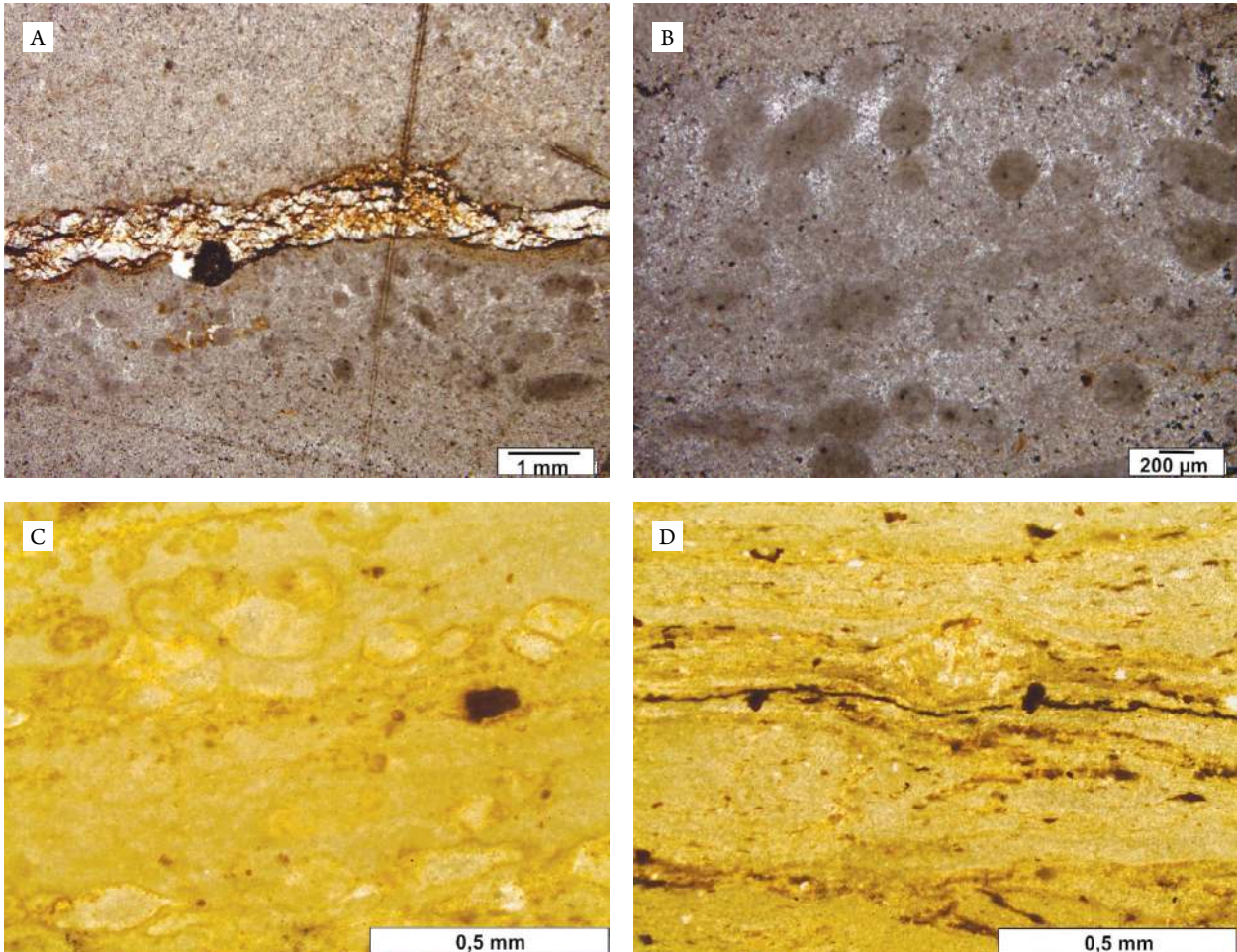


**Figure 10.** Limestone with peloids microfacies: (A), (B) and (C) peloidal level; (D) peloid in the center deforming lamination. Photomicrograph: parallel nicols.

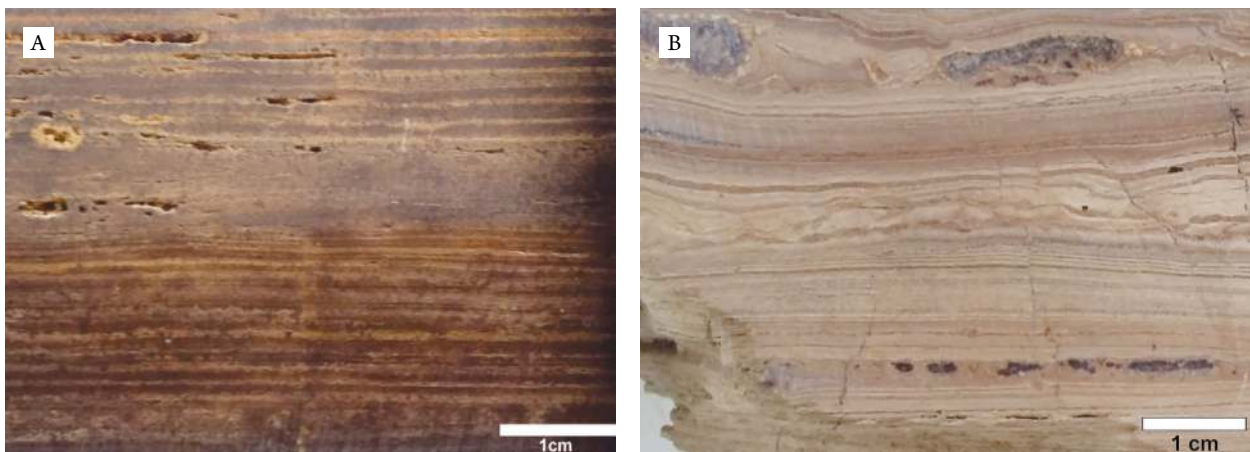


**Figure 11.** Laminated limestone: (A) fenestral and vuggy porosities formed by a dissolution process; (B) vuggy porosity (upper portion) filled with silica, in addition to several shear fractures that displace the laminations of the laminated limestone.

to the increase in pressure (P) and the temperature (T) of the dissolved silica, precipitates later in the pores.

According to Martill *et al.* (2007), the existence of halite pseudomorphs in these limestones indicates that the basin experienced aridity conditions, where hypersalinity prevailed in the deposition period of the laminated limestones. These authors have recognized five types of pseudomorph shapes of halite. Here, only the so-called type 1 is observed, which occurs as a kind of cross and, occasionally, star, in which a series of concentric circles appear in layers of laminated limestone.

Sulfate minerals, as well as evaporites, are generally formed in environments with a low supply of terrigenous material. They begin their precipitation in a dry climate with increased evaporation due to a decrease in the lake level that makes the waters more concentrated and allows the formation of brines.

Evaporites are deposits from arid environments, and, in the case of the Araripe Basin, they are representatives of the Ipubi Formation. Evaporative solutions are highly mobile due to their low density. Evaporites can migrate to adjacent or underlying strata and precipitate as diagenetic sulfates (usually as crystals

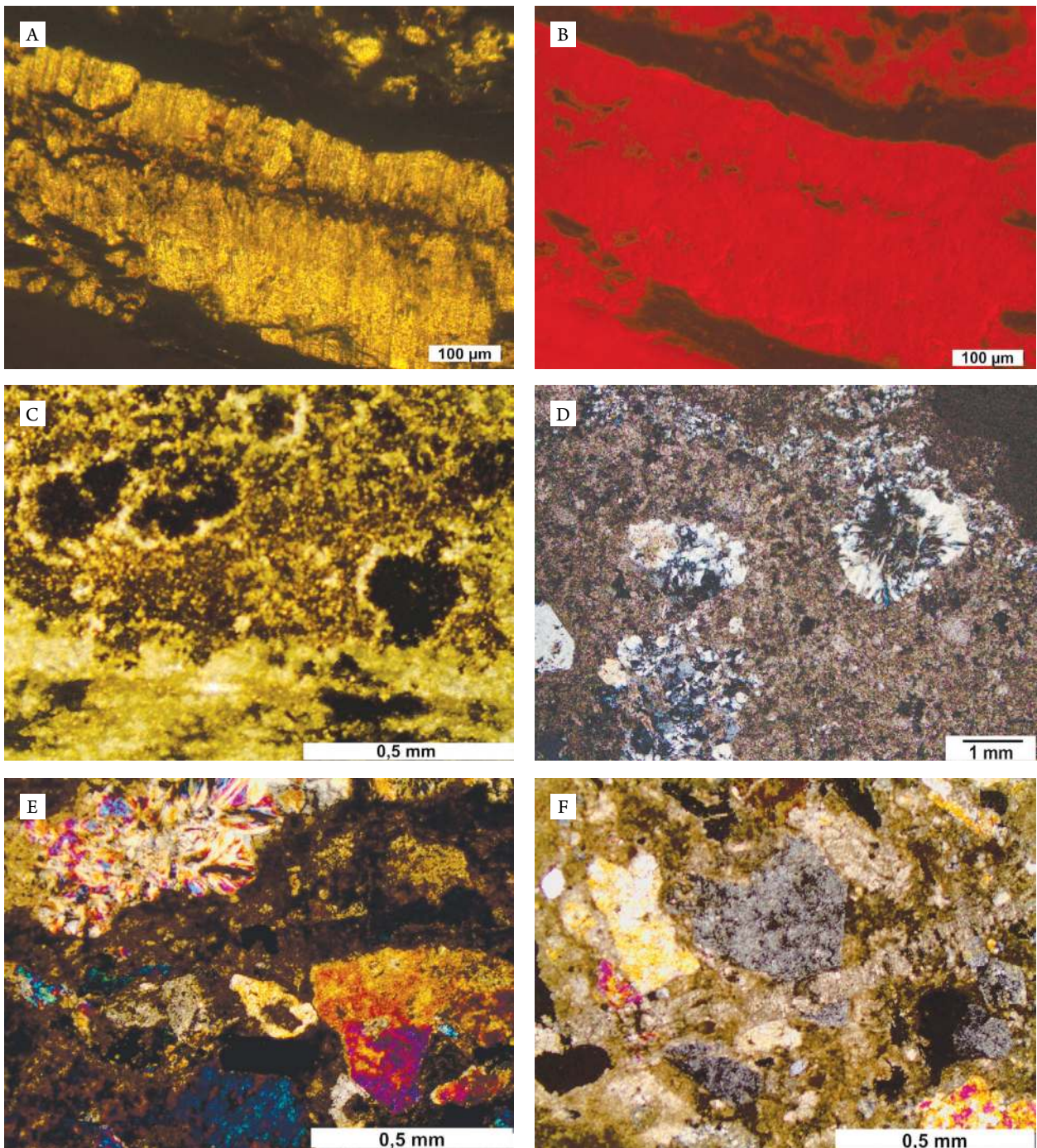


**Figure 12.** (A) Fibrous calcite at parallel nicols; (B) the same image as A where the fibrous calcite shows high luminescence under cathodoluminescence analysis; (C) pyrite occurring in a widespread form, replacing bioclasts (parallel nicols); (D) chalcedony spherulite replacing the micritic matrix (crossed nicols); (E) anhydrite in the upper portion of the image and barite in the lower right portion (crossed nicols); (F) gypsum with gray coloration and anhydrite colored with high birefringence (crossed nicols).

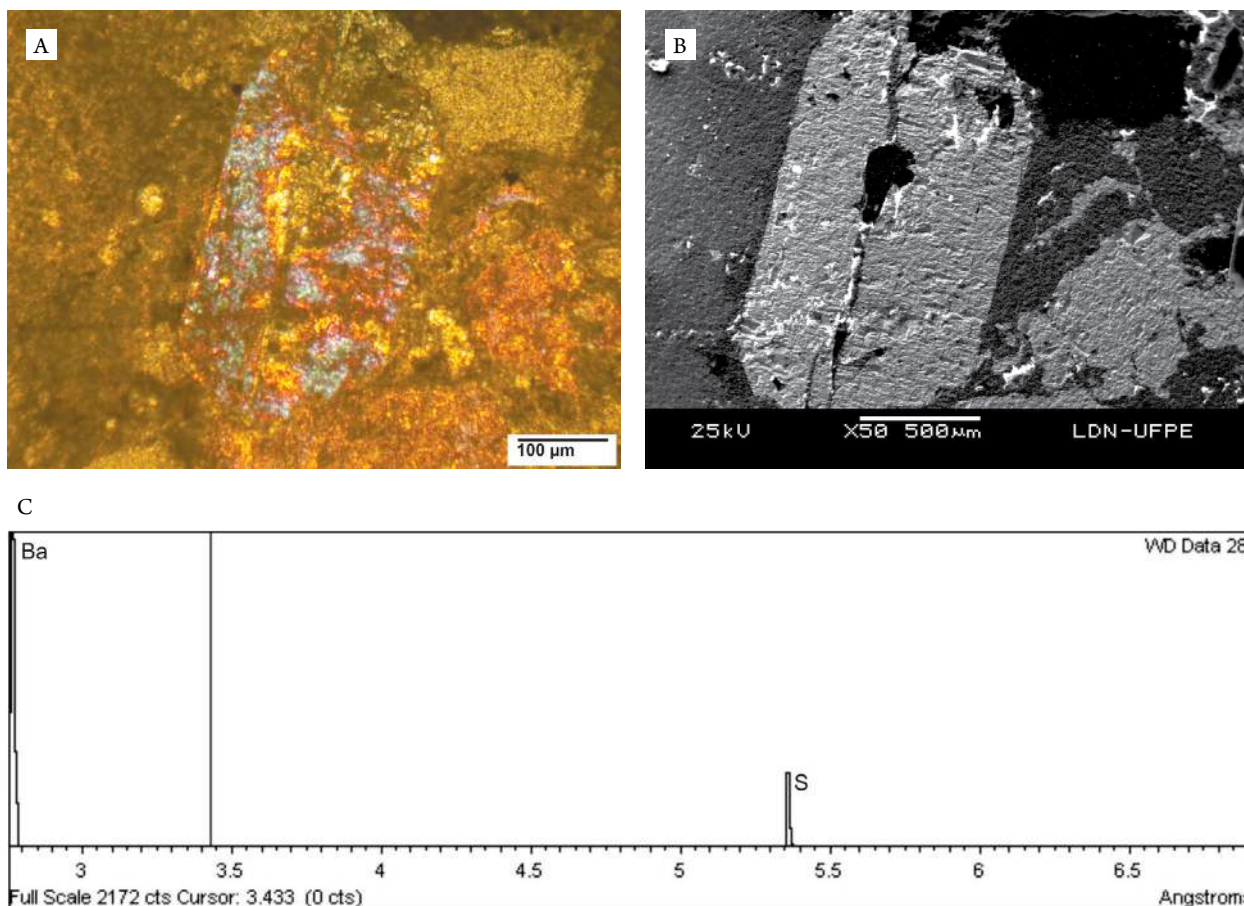


**Figure 13.** (A) Barite crystal under optical microscopy (crossed nicols); (B) barite crystal identified in scanning electron microscopy (SEM) analysis; (C) spectrum by wavelength, in SEM analysis, showing the peaks of the elements barium (Ba) and sulfur (S).

and nodules or as carbonate replacements) in units that may be unrelated to arid environments, such as events occurring in the upper part of the Crato Formation.

## CONCLUSIONS

The laminated limestones in the upper part of the Crato Formation consist mainly of calcilutite with a micritic matrix, framboidal pyrite and iron oxide. The observed paleontological content was ostracods and peloids.

These limestones have secondary porosity. However, it has been found that these porosities are locally filled due to diagenetic processes. Hence, these rocks become less porous.

The processes identified from different diagenetic stages that affect these laminated limestones are cementation, dissolution, replacement, recrystallization and compaction. Additionally, the diagenetic constituents found in the thin sections include calcite, pyrite, silica and sulfates.

From the obtained data, it can be concluded that a large part of the microstructures may be related to local seismicity,

probably related to the reactivation of the Patos Shear Zone. However, they were also generated diagenetically by overload.

In general, these limestones in the upper part of the Crato Formation represent a gradual growth in an arid and salty depositional environment, where silica and sulfates were observed in the upper part in contact with the Ipubi Formation. In addition, algae mats were noted, and the presence of which is also linked to a high salinity environment.

## ACKNOWLEDGMENTS

We acknowledge the financial support for the field work and the analysis from the Brazilian National Council for Scientific and Technological Development (CNPq — Project 440.553/2014-8). We are grateful to the Crato Project (Petrobras/Foundation for Development Support — FADE/UFPE) and Foundation for Science and Technology Support of Pernambuco (FACEPE), for providing research funding. We would also like to thank the editor, Claudio Riccomini, and the anonymous reviewers for their corrections and valuable comments and suggestions.

## ARTICLE INFORMATION

Manuscript ID: 20180097. Received on: 02/18/2018. Approved on: 12/28/2018.

F. A. A. worked the data obtained in the analyses, wrote the first version, improved and making corrections at all stages until the final version of the manuscript. A. C. S. and G. M. S. R. prepared the figures and table. T. S. M. made suggestions and contributed to the geological setting. J. A. B. revised and improved the results and discussions of the manuscript. V. H. M. L. N. provided guidance, revised, improved and made suggestions for the entire manuscript.

Competing interests: The authors declare no competing interests.

## REFERENCES

- Arai M. 2006. Revisão estratigráfica do Cretáceo Inferior das Bacias Interiores do Nordeste do Brasil. *Geociências*, **25**(1):7-15.
- Arai M. 2012. Evidência micropaleontológica da ingressão marinha aptiana (pré- evaporítica) na Bacia do Araripe, Nordeste do Brasil. In: Congresso Brasileiro de Geologia, 46., Santos. *Anais...* São Paulo: Sociedade Brasileira de Geologia.
- Assine M.L. 1990. *Sedimentação e Tectônica da Bacia do Araripe, Nordeste do Brasil*. Dissertation, Instituto de Geociências e Ciências Exatas, Universidade Estadual Paulista "Júlio de Mesquita Filho", Rio Claro.
- Assine M.L. 1992. Análise Estratigráfica da Bacia do Araripe, Nordeste do Brasil. *Revista Brasileira de Geociências*, **22**(3):289-300.
- Assine M.L. 2007. Bacia do Araripe. *Boletim de Geociências da Petrobras*, **15**(2):371-389.
- Assine M.L., Perinotto J.A.J., Custódio M.A., Neumann V.H., Varejão F.G., Mescolotti P.C. 2014. Sequências deposicionais do Andar Alagoas da Bacia do Araripe, Nordeste do Brasil. *Boletim de Geociências da Petrobras*, **22**(1):3-28.
- Bates R.L. & Jackson J.A. (1980) *Glossary of Geology*. Falls Church, Virginia, American Geological Institute. 751 p.
- Bathurst R.G.C. 1986. Carbonate diagenesis and reservoir development: Conservation, destruction and creation of pores. In: Harris P.M., James N.P., Macintyre I.G. (eds.), *Carbonate Depositional Environments, Modern and Ancient*, 81, p. 1-25. Colorado: Colorado School of Mines Press.
- Batten D.J. 2007. Spores and pollen from the Crato Formation: biostratigraphic and palaeoenvironmental implications. In: Martill D.M., Bechly G., Loveridge R.F. (eds.), *The Crato Fossil Beds of Brazil: Window into an Ancient World*. Cambridge, Cambridge University Press, p. 566-573.
- Berthou P.Y., Depeche F., Colin J.P., Filgueira J.B.M., Teles M.S.L. 1994. New data on the ostracods from Crato lithologic units (lower member of the Santana Formation, Latest Aptian- Lower Albian) of the Araripe Basin (Northeastern Brazil). *Acta Geologica Leopoldensia*, **39**(2):539-554.
- Beurlen K. 1962. A Geologia da Chapada do Araripe. *Anais da Academia Brasileira de Ciências*, **34**(2):365-370.
- Boggs Jr. S. 2009. *Petrology of sedimentary rocks*. 2. ed. New York, Cambridge University Press, 600 p.
- Catto B. 2015. *Laminitos Microbiais no Membro Crato (Neoaptiano), Bacia do Araripe, Nordeste do Brasil*. Dissertation, Universidade Estadual Paulista "Júlio de Mesquita Filho", São Paulo, 111 p.
- Catto B., Jahnert R.J., Warren L.V., Varejão F.G., Assine M.L. 2016. The microbial nature of laminated limestones: Lessons from the Upper Aptian, Araripe Basin, Brazil. *Sedimentary Geology*, **341**:304-315. <https://doi.org/10.1016/j.sedgeo.2016.05.007>
- Choquette P.W., Pray L.C. 1970. Geologic nomenclature and classification of porosity in sedimentary carbonates: *American Association of Petroleum Geologists Bulletin*, **54**:207-250.
- Coimbra J.C., Arai M., Carreño A.L. 2002. Biostratigraphy of Lower Cretaceous microfossils from the Araripe Basin, northeastern Brazil. *Geobios*, **35**(6):687-698. [http://dx.doi.org/10.1016/S0016-6995\(02\)00082-7](http://dx.doi.org/10.1016/S0016-6995(02)00082-7)
- Dunham R.J. 1962. Classification of carbonate rocks according to depositional texture. *Memoir AAPG*, **1**:108-121. <https://doi.org/10.1306/M1357>
- Fambrini G.L., Buarque B.V., Menezes-Filho J.A.B., Valença L.M.M., Araújo J.T., Neumann V.H.M.L. 2012. Análise estratigráfica da Formação Abaiara (Neocomiano), Bacia do Araripe, NE do Brasil: implicações para a implantação da fase rift das bacias fanerozoicas brasileiras. In: Congresso Brasileiro de Geologia, 46., Santos. *Anais...*
- Grabau A.W. 1904. On the classification of sedimentary rocks. *American Geologist*, **33**:228-247.
- Hashimoto A.T., App C.J., Soldan A.L., Cerqueira J.R. 1987. O Neo-Alagoas nas Bacias do Ceará, Araripe e Potiguar (Brasil): caracterização estratigráfica e paleoambiental. *Revista Brasileira de Geologia*, **17**(2):118-122.
- Heimhofer U., Ariztegui D., Lenniger M., Hesselbo S.P., Martill D.M., Rios-Netto A.M. 2010. Deciphering the depositional environment of the laminated Crato fossil beds (Early Cretaceous, Araripe Basin, North-eastern Brazil). *Sedimentology*, **57**(2):677-694. <https://doi.org/10.1111/j.1365-3091.2009.01114.x>
- Lima M.R. 1978. *Palinologia da Formação Santana (Cretáceo do Nordeste do Brasil)*. Tese, Universidade de São Paulo, São Paulo, 335 p.
- Lima M.R. 1980. Palinologia da Formação Santana (Cretáceo do nordeste do Brasil). III. Descrição sistemática dos polens da turma Plicates (Subturma Costates). *Ameghiniana*, **17**(1):15-47.
- Martill D.M., Heimhofer U. 2007. Stratigraphy of the Crato Formation. In: Martill D.M., Bechly G., Loveridge R.F. (Eds.), *The Crato Fossil Beds of Brazil – Window into an Ancient World*, p. 25-43. Cambridge, Cambridge University Press.
- Martill D., Loveridge R., Heimhofer U. 2007. Halite pseudomorphs in the Crato Formation (Early Cretaceous, Late Aptian-Early Albian), Araripe Basin, northeast Brazil: further evidence for hypersalinity. *Cretaceous Research*, **28**:613-620. <https://doi.org/10.1016/j.cretres.2006.10.003>
- Miranda T.S. 2015. *Caracterização Geológica e Geomecânica dos Depósitos Carbonáticos e Evaporíticos da Bacia do Araripe, NE do Brasil*. Thesis, Universidade Federal de Pernambuco, Recife, 269 p.
- Nelson R.A. 1987. Fractured reservoir: turning knowledge into practice. *Society Petroleum Engineering Journal*, **39**(4):407-414. <https://doi.org/10.2118/16470-PA>
- Nelson R.A. 2001. *Geologic analysis of naturally fractured reservoirs*. United States: Gulf Professional Publishing, 352 p.
- Neumann V.H.M.L. 1999. *Estratigrafia, Sedimentologia, Geoquímica y Diagenesis de los Sistemas Lacustres Aptienses- Albienses e la Cuenca de Araripe, Noreste de Brasil*. Thesis. Universidade de Barcelona, Barcelona, 244 p.
- Neumann V.H.M.L., Cabrera L. 1999. Una Nueva Propuesta Estratigrafica para la Tectonosecuencia post-rifte de la Cuenca de Araripe, Noreste de Brasil. In: Simpósio Sobre o Cretáceo do Brasil, 5., e Simpósio Sobre el Cretácico de América Del Sur, 1., Serra Negra. *Anais...* Rio Claro: UNESP, p. 279-285.
- Pons D., Berthou P.Y., Campos D.A. 1990. Quelques observations sur la palynologie de l'Aptien Supérieur et l'Albien du Bassin d'Araripe (NE du Brésil). In: Simpósio sobre a Bacia do Araripe e Bacias Interiores do Nordeste, 1., Crato. *Atas...* URCA, p. 241-252.
- Ponte F.C., Appi C.J. 1990. Proposta de revisão da coluna litoestratigráfica da Bacia do Araripe. In: Congresso Brasileiro de Geologia, 36., Natal. *Anais...* Natal: SBG, p. 211-226.
- Ponte F.C., Ponte Filho F.C. 1996. *Estrutura Geológica e Evolução Tectônica da Bacia do Araripe*. Recife, DNPM, 68 p.
- Santos E.J., Nutman A.P., Brito Neves B.B. 2004. Idades SHIRIMP U-Pb do Complexo Sertânia: implicações sobre a evolução tectônica da Zona Transversal, Província Borborema. *Geologia USP (Série Científica)*, **4**(1):1-12. <https://doi.org/10.5327/S1519-874x2004000100001>
- Silva Silva A.L. 2003. *Estratigrafia Física e Deformação do Sistema Lacustre Carbonático Aptiano-Albiano da Bacia do Araripe em Afloramento Seleccionados*. Dissertation, Programa de Pós-Graduação em Geociências, Universidade Federal de Pernambuco, Recife, 118 p.